



Article

# Henrin A: A New Anti-HIV *Ent*-Kaurane Diterpene from *Pteris henryi*

Wan-Fei Li <sup>1,†</sup>, Juan Wang <sup>2,3,†</sup>, Jing-Jie Zhang <sup>1</sup>, Xun Song <sup>2</sup>, Chuen-Fai Ku <sup>2</sup>, Juan Zou <sup>1</sup>, Ji-Xin Li <sup>1</sup>, Li-Jun Rong <sup>4</sup>, Lu-Tai Pan <sup>1,\*</sup> and Hong-Jie Zhang <sup>2,\*</sup>

Received: 17 September 2015; Accepted: 13 November 2015; Published: 24 November 2015

Academic Editor: Ge Zhang

<sup>1</sup> Guiyang College of Traditional Chinese Medicine, Guiyang 550002, China; wanfeier@live.cn (W.-F.L.); zjj523@126.com (J.-J.Z.); zoujuan-729@163.com (J.Z.); lijixinmylove@yeah.net (J.-X.L.)

<sup>2</sup> School of Chinese Medicine, Hong Kong Baptist University, 7 Baptist University Road, Kowloon Tong, Kowloon, Hong Kong, China; juan\_wang2012@163.com (J.W.); kobe24song@126.com (X.S.); faiku2010@hkbu.edu.hk (C.-F.K.)

<sup>3</sup> School of Public Health, Jilin University, Changchun 130021, China

<sup>4</sup> Department of Microbiology and Immunology, College of Medicine, University of Illinois at Chicago, 833 South Wood Street, Chicago, IL 60612, USA; lijun@uic.edu

\* Correspondences: ltpan@sina.cn (L.-T.P.); zhanghj@hkbu.edu.hk (H.-J.Z.);  
Tel./Fax: +86-852-8823-3016 (L.-T.P.); Tel.: +852-3411-2956 (H.-J.Z.); Fax: +852-3411-2461 (H.-J.Z.)

† These authors contributed equally to this work.

**Abstract:** Henrin A (**1**), a new *ent*-kaurane diterpene, was isolated from the leaves of *Pteris henryi*. The chemical structure was elucidated by analysis of the spectroscopic data including one-dimensional (1D) and two-dimensional (2D) NMR spectra, and was further confirmed by X-ray crystallographic analysis. The compound was evaluated for its biological activities against a panel of cancer cell lines, dental bacterial biofilm formation, and HIV. It displayed anti-HIV potential with an IC<sub>50</sub> value of 9.1 μM (SI = 12.2).

**Keywords:** *Pteris henryi*; *ent*-kaurane diterpene; henrin A; bioactivity evaluation; anti-HIV activity

## 1. Introduction

*Ent*-kaurane compounds are members of a class of diterpenes with a four-membered ring system, which are richly found in the *Isodon* genus (Lamiaceae) [1–3]. They have been known for having a variety of biological activities, including anticancer and antibacterial activities [4–6]. Tetracyclic *ent*-kauranes have also been found in the fern plants of the genus *Pteris* (Pteridaceae family), and some of them have demonstrated biological activities [7–13]. Phytochemical and biological investigation of the plants in the genus *Pteris* may produce potentially novel bioactive diterpenes [14,15].

The genus *Pteris* comprises more than 300 species, 66 of which are distributed in China [16]. Few phytochemical studies have been reported for the chemical constituents of the plants in this genus [17]. Our present study focused on the plant species *P. henryi* Chirst, a perennial herb that has been used as an herbal medicine for the treatment of burns and scalds, lissodexis, traumatic hemorrhages, leucorrhoea, and difficulty and pain in micturition [18]. The plant is mainly distributed in the Guizhou and Yunnan provinces, People's Republic of China [19]. In this study, we report the isolation, structural determination, and biological activity evaluation of henrin A (**1**), a new *ent*-kaurane diterpene (Figure 1).

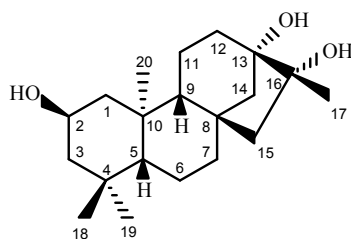


**Figure 1.** Structure of compound henrin A (1).

## 2. Results and Discussion

### 2.1. Compound Identification

The dried leaves of *P. henryi* were extracted with MeOH to afford a MeOH extract, which was separated through silica gel chromatography to yield henrin A (1).

Henrin A (1) was obtained as colorless crystals with UV (MeOH)  $\lambda_{\max}$  (log  $\epsilon$ ) at 204 (1.60) nm (Figure S1). In the IR spectrum, 1 showed absorption of hydroxyl groups (3386, 1099, and 1049  $\text{cm}^{-1}$ ) (Figure S2). Its molecular formula was determined to be  $\text{C}_{20}\text{H}_{34}\text{O}_3$  by means of analyzing its NMR spectroscopic data (Table 1), and further verified by the HR-EIMS data with  $m/z$  345.2405  $[\text{M} + \text{Na}]^+$  (calcd 345.2400) (Figure S3). The molecule of 1 has four double-bond equivalences. However, no carbonyl absorption was observed in the IR spectrum. As evidenced from the  $^1\text{H}$  and  $^{13}\text{C}$  NMR spectral data (Table 1) (Figures S4–S6) as well as the HMQC correlation data (Figure S7), the 20 carbons of compound 1 were characterized as four methyl groups ( $\delta_{\text{H}}$  0.87, 0.93, 1.09, and 1.18 (each 3H, s);  $\delta_{\text{C}}$  19.4 (q), 21.3 (q), 22.8 (q), and 34.2 (q)), an oxy-methine group ( $\delta_{\text{H}}$  3.87 (1H, brtt,  $J = 11.5, 4.3$  Hz);  $\delta_{\text{C}}$  65.4 (d)), two oxy-tertiary carbons ( $\delta_{\text{C}}$  77.4 (s) and 81.1 (s)), eight methylene carbons, two non-oxygenated methine carbons ( $\delta_{\text{H}}$  0.82 (1H, brd,  $J = 11.5$  Hz), and 0.96 (1H, brd,  $J = 7.2$  Hz);  $\delta_{\text{C}}$  57.0 (d) and 57.1 (d)), and three quaternary carbons. No signals were observed in the range of  $\delta_{\text{H}}$  5–7 ppm of the  $^1\text{H}$  NMR spectrum and in the range of  $\delta_{\text{C}}$  90–160 ppm of the  $^{13}\text{C}$  NMR spectrum, indicating that there is no carbon-carbon double-bond in 1. The lack of olefinic signals in the molecule and the calculation of four double-bond equivalences determined that 1 has a tetracyclic-ring system. Compound 1 was thus suggested to have a saturated tetracyclic diterpene having an *ent*-kaurane skeleton.

Through analysis of the long-range correlation data observed in the HMBC (heteronuclear multiple-bond correlation spectroscopy) spectrum (Figure S8), together with the HMQC (heteronuclear multiple-quantum correlation spectroscopy) (Figure S7) and  $^1\text{H}$ - $^1\text{H}$  COSY (correlated spectroscopy) (Figure S9) data (Figure 2), the three oxy-carbon groups (one oxy-methine and two oxy-tertiary carbons) in 1 could be assigned accordingly. Starting from the singlet signals of the methyl protons at C-18 and C-19 ( $\delta_{\text{H}}$  0.93 (H<sub>3</sub>-18), 0.87 (H<sub>3</sub>-19)), the  $^{13}\text{C}$  NMR at  $\delta_{\text{C}}$  51.9 (t) was assigned to C-3 due to the presence of its HMBC correlations to the two methyl protons, which in turn suggested the oxy-methine group at C-2 due to the presence of the  $^1\text{H}$ - $^1\text{H}$  COSY correlations between H-2 ( $\delta_{\text{H}}$  3.87) and H<sub>2</sub>-3 ( $\delta_{\text{H}}$  1.07 and 1.72). The presence of the HMBC correlations of the singlet signals of the methyl protons at C-17 ( $\delta_{\text{H}}$  1.18) to both oxy-tertiary carbons at  $\delta_{\text{C}}$  77.4 and 81.1 suggested that both C-13 and C-16 were substituted with a hydroxy group, respectively.

In the ROESY (rotating frame nuclear Overhauser effect spectroscopy) spectrum (Figure S10), the presence of the ROE (rotating frame Overhauser effect) correlations (Figure 3) of H-2 ( $\delta_{\text{H}}$  3.87) with H<sub>2</sub>-20 suggested the hydroxy group of C-2 to be  $\beta$ -oriented. In addition, the presence of the ROE correlations of H-5 ( $\delta_{\text{H}}$  0.82) to H<sub>3</sub>-18 and the lack of ROE cross-peaks of H-5 to H-2 and H<sub>3</sub>-19 suggested H-5 to be  $\beta$ -oriented. Furthermore, the  $\beta$ -orientation of H-9 ( $\delta_{\text{H}}$  0.96) was deduced on the basis of the observation of the ROE correlation of H-9 with H-5 and the lack of ROE correlation between H-9 and H<sub>3</sub>-20.

**Table 1.**  $^1\text{H}$  and  $^{13}\text{C}$  NMR data of compound **1**<sup>a</sup>.

No.	$\delta_{\text{H}}$ (mult, $J$ in Hz) <sup>b</sup>	$\delta_{\text{C}}$ (mult) <sup>c</sup>	No.	$\delta_{\text{H}}$ (mult, $J$ in Hz) <sup>b</sup>	$\delta_{\text{C}}$ (mult) <sup>c</sup>
1 $\alpha$	2.15 (brddd, 12.0, 3.8, 1.9)	50.3 t	11 $\alpha$	1.65 (overlap)	20.7 t
1 $\beta$	0.67 (brt, 11.7)	-	11 $\beta$	1.82 (overlap)	-
2 $\alpha$	3.87 (brtt, 11.5, 4.3)	65.4 d	12 $\alpha$	1.68 (overlap)	34.6 t
3 $\alpha$	1.72 (brddd, 12.5, 4.3, 1.9)	51.9 t	12 $\beta$	1.64 (overlap)	-
3 $\beta$	1.07 (brt, 12.0)	-	13	-	77.4 s
4	-	35.7 s	14 $\alpha$	1.66 (overlap)	44.0 t
5 $\beta$	0.82 (brd, 11.5)	57.0 d	14 $\beta$	1.83 (d, 11.9)	-
6 $\alpha$	1.34 (brqd, 12.1, 1.9)	21.2 t	15 $\alpha$	1.50 (dd, 14.5, 1.3)	56.7 t
6 $\beta$	1.59 (brd, 12.3)	-	15 $\beta$	1.63 (d, 14.7)	-
7 $\alpha$	1.60 (overlap)	43.2 t	16	-	81.1 s
7 $\beta$	1.44 (brtd, 11.9, 3.4)	-	17	1.18 (s)	21.3 q
8	-	42.2 s	18	0.93 (s)	34.2 q
9 $\beta$	0.96 (brd, 7.2)	57.1 d	19	0.87 (s)	22.8 q
10	-	41.9 s	20	1.09 (s)	19.4 q

<sup>a</sup> Data were recorded in  $\text{CD}_3\text{OD}$ ;  $\delta$  values are given in ppm with reference to the signal of  $\text{CD}_3\text{OD}$  ( $\delta$  3.31 ppm) for  $^1\text{H}$  and to the center peak of the signal of  $\text{CD}_3\text{OD}$  ( $\delta$  49.0 ppm) for  $^{13}\text{C}$ ; <sup>b</sup> Multiplicities in parentheses represent: s (singlet), brs (broad singlet), dd (doublet of doublet), brdd (broad doublet of doublet), brtd (broad triplet of doublet), brqd (broad quartet of doublet), ddd (doublet of doublet of doublet), brddd (broad doublet of doublet of doublet), t (triplet), brt (broad triplet), and brtt (broad triplet of triplet); <sup>c</sup> Multiplicities represent: s (quaternary carbon), d (CH), t ( $\text{CH}_2$ ), and q ( $\text{CH}_3$ ).

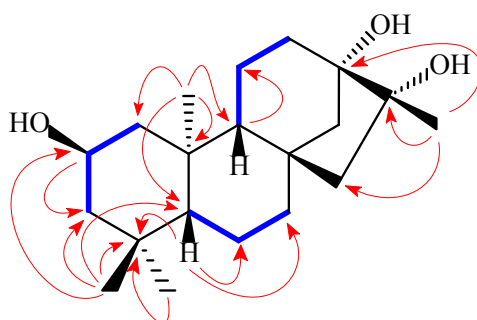


**Figure 2.** Key COSY (marked as blue bold bonds (H—H)) and HMBC (the red arrows (H—C)) correlations for compound **1**.

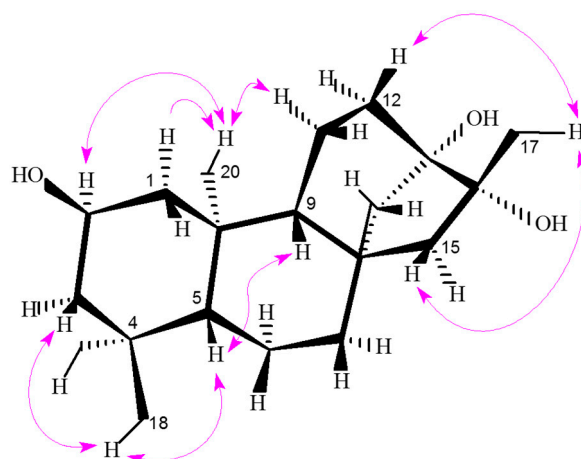


**Figure 3.** Key ROESY correlations (indicated as magenta arrows (H—H)) for compound **1**.

To further confirm the chemical structure, compound **1** was crystallized in MeOH to afford a colorless crystal with the monoclinic space group of  $\text{P}2_12_12_1$ , which was analyzed by X-ray

crystallography. Through structural refinement [20,21], the chemical structure of **1** was confirmed as shown in Figure 4. Like the *Isodon* plants, the diterpenes produced by the ferns in the genus *Pteris* are all *ent*-kaurane diterpenes [7–13]. Compound **1** is also an *ent*-kaurane diterpene due to the observation of the negative optical rotation ( $[\alpha]_D^{11} - 5.66^\circ$ ) as well as the consideration of the similar biogenetic pathways used by the *Pteris* plants for producing the same class of congeners [22–24]. Accordingly, **1** was determined to be *ent*-2 $\beta$ , 13 $\alpha$ , 16 $\alpha$ -trihydroxy-kaurane, and given the trivial name of henrin A.

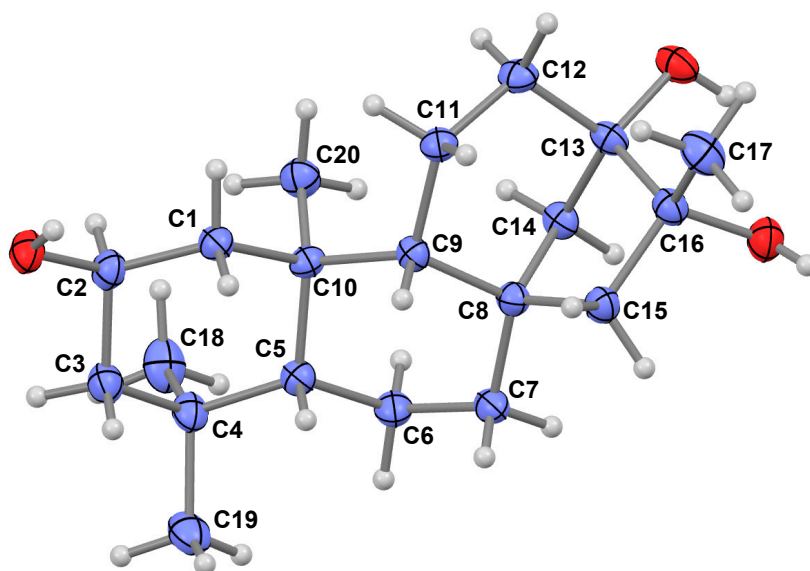


**Figure 4.** ORTEP (oak ridge thermal ellipsoid plot program) drawing of compound **1** (Blue ball: carbon; grey ball: hydrogen; red ball: oxygen).

## 2.2. Biological Activity

Henrin A (**1**) was evaluated for its cytotoxic activity against a panel of human cancer cell lines comprising KB (cervical), HCT116 (colon), A549 (lung), and MCF-7 (breast) cell lines. No inhibitory activity against these cell lines was observed for **1** at a concentration of 20  $\mu\text{g}/\text{mL}$ . Due to the low cytotoxicity of the compound, **1** was further evaluated for its antimicrobial potential.

The dental biofilm formation inhibitory as well as the antifungal activity assays (Table 2) determined that **1** had no antimicrobial activity against the two dental pathogens *Streptococcus mutans* and *S. sobrinus* at a concentration of 20  $\mu\text{g}/\text{mL}$ . Compound **1** was also evaluated for its antifungal activity against the athlete's foot fungus *Trichophyton rubrum*. No antifungal inhibitory activity was observed for this compound at a concentration of 20  $\mu\text{g}/\text{mL}$  (Table 2).

**Table 2.** Antimicrobial activity of henrin A (**1**) against biofilm of two dental bacteria and the athlete's foot fungus.

Compounds	Growth Inhibition Rate (%)		
	Bacterial Biofilm Formation		Fungus
	<i>S. mutans</i>	<i>S. sobrinus</i>	<i>T. rubrum</i>
Henrin A ( <b>1</b> ) <sup>a</sup>	15.55 $\pm$ 5.66	11.20 $\pm$ 2.23	9.73 $\pm$ 8.75
Penicillin G <sup>b</sup>	80.44 $\pm$ 3.14	76.82 $\pm$ 3.93	-
Chlorhexidine <sup>c</sup>	77.26 $\pm$ 6.30	71.49 $\pm$ 5.21	83.12 $\pm$ 0.47
Miconazole <sup>a</sup>	-	-	80.69 $\pm$ 0.10

<sup>a</sup> Compound assay concentration at 20  $\mu\text{g}/\text{mL}$ ; <sup>b</sup> Compound assay concentration at 10  $\mu\text{g}/\text{mL}$ ; <sup>c</sup> Compound assay concentration at 12  $\mu\text{g}/\text{mL}$ .

Henrin A (**1**) was then evaluated for its anti-HIV activity using our previously established “One-Stone-Two-Birds” assay evaluation system [25]. This protocol allows us to identify potential inhibitors for HIV replication (post-entry steps). This protocol is an easy, safe, and efficient HIV vector-based assay system to evaluate and identify potential inhibitors against HIV replication (Figure 5 and Table 3). Henrin A (**1**) was found to exhibit anti-HIV activity with an  $IC_{50}$  value of 9.1  $\mu\text{M}$  with selective index of 12.2.

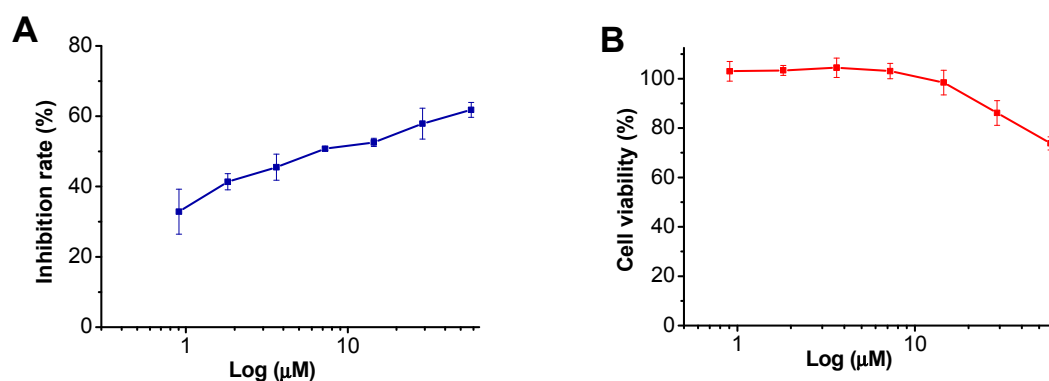


**Figure 5.** Inhibition of HIV/VSV-G by compound **1**. (A) The inhibitory effect of **1** on HIV/VSV-G infectivity was investigated, and it displayed dose-dependent inhibitory activities; (B) The cytotoxicity of **1** was tested on A549 target cells. Three independent experiments were performed to determine the effect of the compound.

**Table 3.** Anti-HIV activity of compound **1**.

Compound	$IC_{50}$ ( $\mu\text{M}$ )	$CC_{50}$ ( $\mu\text{M}$ )	SI
Henrin A	9.1	110.5	12.2
AZT (zidovudine)	0.03	>100	>3333

Many kaurane compounds have been found to possess cytotoxic activity due to the presence of an  $\alpha$ ,  $\beta$ -unsaturated ketone group in their structures [26]. However, for those without this structural feature, low or no cytotoxicity activity is expected [27–30], and these compounds thus may be further explored for their antimicrobial potential. Henrin A (**1**) is an *ent*-kaurane diterpene belonging to this category, and our assay determined that this compound was not toxic against a panel of human cell lines but indeed displayed anti-HIV activity. More than 1000 different types of *ent*-kaurane compounds have been discovered from plants [30]. These diterpenes can be a valuable source for the discovery of antiviral agents by testing the natural or modified compounds without an  $\alpha$ ,  $\beta$ -unsaturated ketone group.

### 3. Experimental Section

#### 3.1. General Experimental Procedures

Optical rotation was measured with a Rudolph digital polarimeter. IR spectrum was recorded on a VECTOR22 spectrophotometer (Bruker, Rheinstetten, Germany) with KBr pellets. 1D (one dimensional) and 2D (two dimensional) NMR spectra were recorded on a JEOL 500MHz spectrometer (JEOL Ltd., Tokyo, Japan). Unless otherwise specified, chemical shifts ( $\delta$ ) were expressed in ppm with reference to the solvent signals. High-resolution mass spectrum (HR-EIMS) was performed on a VG Autospec-3000 spectrometer (VG, Manchester, UK) under 70 eV. Column chromatography was performed with silica gel (200–300 mesh; Qingdao Marine Chemical, Inc., Qingdao, China). Fractions were monitored by TLC and spots were visualized by heating silica gel plates sprayed with 10%  $\text{H}_2\text{SO}_4$  in EtOH. All solvents including petroleum ether (60–90  $^\circ\text{C}$ ) were distilled prior to use.

### 3.2. Plant Material

The plant materials of the leaves of *P. henryi* Chirst were collected in Anshun, Guizhou Province, China, in September 2010. The voucher specimen was identified by Professor Junhua Zhao of the Guiyang College of Traditional Chinese Medicine, and deposited at Guiyang College of Traditional Chinese Medicine, with the number of the voucher specimen as No. 20101003.

### 3.3. Extraction and Isolation

The air-dried powder of the leaves of *P. henryi* Chirst (5 kg) was percolated with 95% MeOH at room temperature (3 × 5 L), and the MeOH crude extract (266 g) was subjected to silica gel chromatography separation (10 cm × 100 cm), eluting with a gradient solvent system of CHCl<sub>3</sub>/MeOH (from 10/1 to 0/1, *v/v*) to afford six fractions (A–F). Fraction C was separated over an additional chromatographic column of silica gel (30 mm × 300 mm), eluting with a gradient solvent system of CHCl<sub>3</sub>/MeOH (from 5/1 to 1/1, *v/v*) to afford fraction G, which was further separated by a Sephadex LH-20 column (300 mm × 1000 mm), eluting with the solvent CHCl<sub>3</sub>/MeOH (1/1, *v/v*) to afford herin A (30 mg).

Henrin A (1): Colorless crystals (MeOH); mp 246–248 °C;  $[\alpha]_D^{11} - 5.66^\circ$  (*c* 2.12, MeOH); UV (MeOH)  $\lambda_{\max}$  (log  $\epsilon$ ) 204 (1.60) nm; IR (KBr)  $\nu_{\max}$  3386, 2940, 2865, 1447, 1468, 1334, 1146, 1099, 1049, 601 cm<sup>-1</sup>; <sup>1</sup>H and <sup>13</sup>C NMR, see Table 1; HR-EIMS ( $[M]^+$  *m/z* 345.2405  $[M + Na]^+$  (calcd. 345.2400 for C<sub>20</sub>H<sub>34</sub>O<sub>3</sub>Na)).

### 3.4. X-ray Data of Henrin A (1)

CCDC 1039988 contains the supplementary crystallographic data for this paper. These data can be obtained free of charge from The Cambridge Crystallographic Data Centre (Available online: [www.ccdc.cam.ac.uk/data\\_request/cif](http://www.ccdc.cam.ac.uk/data_request/cif)). Crystal data of **1** (from MeOH): space group P2<sub>1</sub>2<sub>1</sub>2<sub>1</sub>, C<sub>20</sub>H<sub>34</sub>O<sub>3</sub>, *M* = 322.25, *a* = 6.462(2) Å, *b* = 12.320(4) Å, *c* = 22.311(7) Å,  $\alpha = \beta = \gamma = 90.00^\circ$ , *V* = 1776.3(9) Å<sup>3</sup>, *T* = 293(2) K, *Z* = 4.  $\mu$  (Mo *K* $\alpha$ ) = 0.71073 mm<sup>-1</sup>. A crystal of dimensions of 0.26 mm × 0.25 mm × 0.24 mm was used for measurements on an APEX DUO diffractometer (Bruker, Rheinstetten, Germany) with a graphite monochromator ( $\omega$ - $\kappa$  scans,  $2\theta_{\max} = 50.00^\circ$ ), Mo *K* $\alpha$  radiation. The total number of independent reflections measured was 3113, of which 2250 were observed ( $|F|^2 \geq 2\sigma|F|^2$ ). The crystal structure was solved and refined by the direct method SHELXS-97 [31], expanded using difference Fourier techniques and full-matrix least-squares calculations. Final indices: *R*1 = 0.0601, *wR*2 = 0.1458 (*w* = 1/ $\sigma|F|^2$ ), *s* = 1.062. Flack parameter = -0.3(2).

### 3.5. Biological Activity of Henrin A (1)

#### 3.5.1. Cytotoxicity Assay

Cytotoxicity assays involving oral epidermoid (KB: a Hela derivative previously referred as oral epidermis), colon (HCT116), breast (MCF-7), and lung (A549) carcinoma cell lines (ATCC, Manassas, VA, USA) were performed using sulforhodamine B based on the slightly modified protocols used for individual cell lines [32]. KB and A549 cells were maintained in Dulbecco's modified Eagle's medium (DMEM) (Life Technologies, Carlsbad, CA, USA). HCT116 cells were maintained in McCoy's 5A medium (Life Technologies). MCF-7 cells were maintained in DMEM medium containing 10 mg/L of insulin. Briefly, medium was supplemented with 10% fetal bovine serum (FBS) (Life Technologies). Serial dilutions of test samples were prepared using 10% aqueous DMSO as solvent. The cell suspension was added into 96-well microliter plates in 190  $\mu$ L at plating densities of 5000 cells/well. One plate was fixed *in situ* with TCA to represent a no growth control at the time of drug addition (day 0). Then 10  $\mu$ L 10% aqueous DMSO was used as control group. After 72 h incubation, the cells were fixed to plastic substratum by the addition of 50  $\mu$ L cold 50% aqueous trichloroacetic acid and washed with water after incubation at 4 °C for 30 min. After staining cells with 100  $\mu$ L of 0.4%

sulforhodamine B in 1% aqueous AcOH for 30 min, unbound dye was removed by washing four times with 1% aqueous AcOH. Allowed the plates to dry at room temperature, then the bound dye was solubilized with 200  $\mu$ L 10 mM unbuffered Tris base, pH 10. Shaken for 5 min or until the dye was completely solubilized and the optical density was measured at 515 nm using an ELISA plate reader (Bio-Rad, Hercules, CA, USA). The average data were expressed as a percentage, relative to the control. Percentage growth inhibition was calculated as:  $(OD(\text{cells} + \text{samples}) - OD(\text{day 0 only cells})) / (OD(\text{cells} + 10\% \text{ DMSO}) - OD(\text{day 0 only cells})) = \% \text{ survival}$ , Cytotoxicity =  $1 - \% \text{ survival}$ .

### 3.5.2. Anti-Biofilm Activity Test

The anti-dental bacterial activity was evaluated against *Streptococcus mutans* (ATCC35668) and *S. sobrinus* (ATCC33478) (both strains were obtained from Rory Munro Watt's laboratory of Faculty of Dentistry, Hong Kong University, Hong Kong), and the antifungal activity was evaluated against *Trichophyton rubrum* (ATCC MYA-4438) (obtained from Institute of Dermatology, Chinese Academy of Medical Science, Nanjing, China). Biofilm formation was quantified according to a method previously described [33], with minor modifications. Briefly, the bacteria were suspended in BHI broth until turbidity was equal to a 0.5 McFarland Standard [34], and then bacterial suspension was diluted 1:100 into fresh BHI broth in microtiter wells (SPL Lifesciences Co., Gyeonggi-do, Korea) supplemented with the compound at a final concentration of 20  $\mu$ g/mL or with penicillin G, chlorhexidine, and DMSO as the two positive and one negative controls, respectively. After 24 h of incubation at 37 °C without agitation, the content of each well was removed, and each well was washed three times with 250  $\mu$ L of sterile physiological saline. The plates were vigorously shaken in order to remove all non-adherent bacteria. The remaining attached bacteria were fixed with 200  $\mu$ L of methanol per well, and after 15 min plates were emptied and left to dry. Then, 50  $\mu$ L of the crystal violet solution (1%, *wt/vol*) was added to each sample well, and the mixture was incubated at room temperature for 15 min. Wells were washed four times with distilled water and were filled with 200  $\mu$ L of 95% ethanol to solubilize crystal violet in the solvent. The eluent (150  $\mu$ L) was transferred to a new microtiter well, and the absorbance was determined with a multimode microplate reader (Bio-Rad) at 570 nm.

### 3.5.3. Antifungal Microtiter Assay

A 96-flat-bottom-well microtiter plate (SPL Lifesciences Co., Gyeonggi-do, Korea) was used in experiments to evaluate the effectiveness of the compound in inhibiting *T. rubrum*. The antifungal activity tests were performed using the broth micro dilution method as described in M38-A2, with modifications [35,36]. The medium used was Roswell Park Memorial Institute medium (RPMI) 1640 (Life Technologies Inc., Grand Island, NE, USA) with L-glutamine buffered to pH 7.0 with 0.165 M morpholinepropanesulfonic acid (MOPS), supplemented with 2% glucose. The cell suspension was prepared in growth medium. Each test well received 190  $\mu$ L of conidia at  $2.0 \times 10^4$  /mL, and 10  $\mu$ L of the compound solution at 4 mg/mL, where the final concentrations in the well were 20  $\mu$ g/mL. Positive (10  $\mu$ L of miconazole with 190  $\mu$ L of inoculum) and negative (200  $\mu$ L of medium) controls were included in all experiments. The plates were incubated at 30 °C for 72 h. Then, 20  $\mu$ L 5 mg/mL 3-(4,5-dimethylthiazol-2-yl)-2, 5-diphenyltetrazolium bromide (MTT) was added into the 96-well plate, then cultured 10 more hours. The plate was centrifuged at 2500 rpm for 10 min. Remove the supernatant and add 150  $\mu$ L DMSO to dissolve the formazan by shaking for 30 min. The 96-well plate was centrifuged and the supernatant was transferred to a new 96-well plate, and OD reading was measured at 510 nm by using the microplate reader (Bio-Rad).

### 3.5.4. Inhibitory HIV Activity Assay

HIV/VSV-G were produced by co-transfecting 3  $\mu$ g of VSV-G envelope expression plasmid with 21  $\mu$ g of a replication-defective HIV vector (pNL4-3.Luc.R●E) [37,38] into human embryonic kidney 293T cells (90% confluent) in 10 cm plates with PEI (polyethylenimine) (Invitrogen, Carlsbad, CA, USA), as previously described [26]. Eight hours post-transfection, all media was replaced with

fresh, complete DMEM. Forty-eight hours post-transfection, the supernatants were collected and filtered through a 0.45- $\mu\text{m}$ -pore-size filter (Millipore, Billerica, MA, USA) and the pseudovirions were directly used for infection.

Target A549 cells were seeded at  $10^4$  cells per well (96-well plate) in complete DMEM. Ten microliter compound for serial concentrations (20, 10, 5, 2.5, 1.25, 0.625, and 0.3125  $\mu\text{g}/\text{mL}$ ) and 190  $\mu\text{L}$  of the pseudovirus were incubated with target cells. Forty-eight hours post-infection, cells were lysed and prepared for luciferase assay (Promega, Madison, WI, USA).

#### 4. Conclusions

A new *ent*-kaurane diterpene (henrin A, **1**) was isolated from the leaves of *P. henryi*. The chemical structure was elucidated by analysis of the spectroscopic data and was further confirmed by the X-ray crystallographic analysis. The compound was evaluated for its biological activities against a panel of cancer cell lines, dental bacterial biofilm formation, and HIV. Our assay results showed that henrin A (**1**) had low cytotoxicity due to its lack of an  $\alpha,\beta$ -unsaturated ketone group in the structure, but the compound has been determined as a potential anti-HIV agent in our antiviral assay study.

**Supplementary Materials:** Supplementary materials can be found at <http://www.mdpi.com/1422-0067/16/11/26071/s1>.

**Acknowledgments:** The work described in this paper was collaborative efforts within multi-disciplinary cooperative programs supported by grants from by the Natural Science Foundation Committee of China (81160496), the Science and Technology Fund of Guizhou Province (No. [2009]2145), the Research Grants Council of the Hong Kong Special Administrative Region, China (Project No. HKBU 262912 and HKBU12103014), HKBU Interdisciplinary Research Matching Scheme (RC-IRMS/12-13/03), and Faculty Research Grants, Hong Kong Baptist University (FRG2/14-15/047 and FRG1/13-14/029).

**Author Contributions:** Wan-Fei Li and Juan Zou performed most of the chemistry-related experiments including separation, structure determination of the reported compound with support of Lu-Tai Pan and Jing-Jie Zhang; Juan Wang, Xun Song and Chuen-Fai Ku performed most of the biology-related experiments including cytotoxic activity and antimicrobial evaluation with support of Hong-Jie Zhang and Li-Jun Rong; Lu-Tai Pan and Ji-Xin Li collected the plant materials; Lu-Tai Pan and Jing-Jie Zhang designed the separation study; Hong-Jie Zhang and Li-Jun Rong designed the bioassay study; Wan-Fei Li, Lu-Tai Pan and Hong-Jie Zhang co-wrote the manuscript with the assistance of Jing-Jie Zhang and Li-Jun Rong. All authors discussed the results and commented on the manuscript.

**Conflicts of Interest:** The authors declare no conflict of interest.

#### References

1. Huang, S.X.; Xiao, W.L.; Li, L.M.; Li, S.H.; Zhou, Y.; Ding, L.S.; Lou, L.G.; Sun, H.D. Bisrubescensins A–C: Three new dimeric *ent*-kauranoids isolated from *Isodon rubescens*. *Org. Lett.* **2006**, *8*, 1157–1160. [[CrossRef](#)] [[PubMed](#)]
2. Sun, H.D.; Xu, Y.L.; Jiang, B. *Diterpenoids from Isodon Species*; SciPress, Ltd.: Beijing, China, 2001.
3. Sun, H.D.; Huang, S.X.; Han, Q.B. Diterpenoids from *Isodon* species and their biological activities. *Nat. Prod. Rep.* **2006**, *23*, 673–698. [[CrossRef](#)] [[PubMed](#)]
4. Chen, S.; Gao, J.; Halicka, H.D.; Huang, X.; Traganos, F.; Darzynkiewicz, Z. The cytostatic and cytotoxic effects of oridonin (Rubescenin), a diterpenoid from *Rabdosia rubescens*, on tumor cells of different lineage. *Int. J. Oncol.* **2005**, *26*, 579–588. [[CrossRef](#)] [[PubMed](#)]
5. Wang, S.P.; Zhong, Z.F.; Wan, J.B.; Tan, W.; Wu, G.S.; Chen, M.W.; Wang, Y.T. Oridonin induces apoptosis, inhibits migration and invasion on highly-metastatic human breast cancer cells. *Am. J. Chin. Med.* **2013**, *41*, 177–196. [[CrossRef](#)] [[PubMed](#)]
6. Ikezoe, T.; Yang, Y.; Bandobashi, K.; Saito, T.; Takemoto, S.; Machida, H.; Togitani, K.; Koeffler, H.P.; Taguchi, H. Oridonin, a diterpenoid purified from *Rabdosia rubescens*, inhibits the proliferation of cells from lymphoid malignancies in association with blockade of the NF- $\kappa$ B signal pathways. *Mol. Cancer Ther.* **2005**, *4*, 578–586. [[CrossRef](#)] [[PubMed](#)]
7. Fujii, K.; Xu, H.J.; Tatsumi, H.; Imahori, H.; Ito, N.; Node, M.; Inaba, M. Design and synthesis of antitumor compounds based on the cytotoxic diterpenoids from the genus *Rabdosia*. *Chem. Pharm. Bull.* **1991**, *39*, 685–689. [[CrossRef](#)] [[PubMed](#)]



8. Murakami, T.; Maehashi, H.; Tanaka, N.; Satake, T.; Kuraishi, T.; Komazawa, Y.; Saiki, Y.; Chen, C.M. Chemical and chemotaxonomical studies on filices. LV. Studies on the constituents of several species of *Pteris*. *Yakugaku Zasshi* **1985**, *105*, 640–648.
9. Murakami, T.; Iida, H.; Tanaka, N.; Saiki, Y.; Chen, C.M.; Iitaka, Y. Chemical and chemotaxonomic study of filicales. 33. Chemical studies of the components of *Pteris longipes* Don. *Chem. Pharm. Bull.* **1981**, *29*, 657–662. [[CrossRef](#)]
10. Liu, Q.F.; Qin, M.Z. Chemical studies of the components of *Pteris multifida* Poir. *Chin. Tradit. Herb. Drugs (Zhong Cao Yao)* **2002**, *33*, 113–114.
11. Tanaka, N.; Hata, M.; Murakami, T.; Saiki, Y.; Chen, C.M. Chemical and chemotaxonomic studies of *Pteris* and related genera (Pteridaceae). XIII. Additional components of *Pteris dispar* Kunze. *Chem. Pharm. Bull.* **1976**, *24*, 1965–1966. [[CrossRef](#)]
12. Murakami, T.; Tanaka, N.; Komazawa, Y.; Saiki, Y.; Chen, C.M. Chemical and chemotaxonomic studies of ferns. XLI. Additional contents of *Pteris purpureorachis* Copel. *Chem. Pharm. Bull.* **1983**, *31*, 1502–1504. [[CrossRef](#)]
13. Tanaka, N.; Murakami, T.; Saiki, Y.; Chen, C.M.; Iitaka, Y. Chemical and chemo taxonomic study of filices. XXXIV. chemical studies of the components of *Pteris purpureorachis* Copel. *Chem. Pharm. Bull.* **1981**, *29*, 663–666. [[CrossRef](#)]
14. Zhang, X.; Li, J.H.; He, C.W.; Tanaka, N. Study on the diterpenoid constituents and anticancer action of *Pteris semipinnata*. *Chin. Pharm. J.* **1999**, *34*, 512–514.
15. Cheng, H.E.; Liang, N.; Li, M.O. Inhibitory effect of compound 6F isolated from *Pteris semipinnata* L. on biosynthesis of DNA, RNA and protein in HL-60 cells. *J. Guangdong Med. Coll.* **2002**, *20*, 247–250.
16. Zhu, Y.L.; Song, L.D. The research of *Pteris* genus in China. *China Prac. Med.* **2014**, *9*, 256.
17. Murakami, T.; Tanaka, N. Occurrence, structure and taxonomic implications of fern constituents. In *Fortschritte der Chemie organischer Naturstoffe/Progress in the Chemistry of Organic Natural Products*; Herz, W., Grisebach, H., Kirby, G.W., Tamm, C., Eds.; Springer Vienna: Tokyo, Japan, 1988; pp. 1–310.
18. The Editorial Committee of Flora of Guizhou. *Flora of Guizhou (Guizhou Zhiwu Zhi Volume 8)*; Guizhou People Press: Guiyang, China, 1986; pp. 491–492.
19. Pan, L.T.; Zhao, J.H.; Sun, Q.W. *Medicinal Pteridophytes of Guizhou (Guizhou Juelei Zhiwu zhi)*; Guizhou Science and Technology Press: Guiyang, China, 2012; p. 113.
20. Flack, H.D. On enantiomorph-polarity estimation. *Act. Crystallogr.* **1983**, *A39*, 876–881. [[CrossRef](#)]
21. Flack, H.D.; Bernardinelli, G. The use of X-ray crystallography to determine absolute configuration. *Chirality* **2008**, *20*, 681–690. [[CrossRef](#)] [[PubMed](#)]
22. Hanson, J.R. The tetracyclic diterpenes. In *International Series of Monographs in Organic Chemistry*; Pergamon Press: London, UK, 1968; Volume 9, p. 8.
23. Huang, S.X. Tetracyclic diterpenes. In *Chemistry of Diterpenes*; Sun, H.D., Ed.; Chemical Industry Press: Beijing, China, 2011; pp. 203–227.
24. Dewick, P.M. *Medicinal Natural Products, A Biosynthetic Approach*; John Wiley & Sons Ltd.: West Sussex, UK, 2009; pp. 228–229.
25. Rumschlag-Booms, E.; Zhang, H.J.; Soejarto, D.D.; Fong, H.H.; Rong, L.J. Development of an antiviral screening protocol: One-Stone-Two-Birds. *J. Antivir. Antiretrovir.* **2011**, *3*, 8–10. [[CrossRef](#)] [[PubMed](#)]
26. Rosselli, S.; Bruno, M.; Maggio, A.; Bellone, G.; Chen, T.H.; Bastow, K.F.; Lee, K.H. Cytotoxic activity of some natural and synthetic *ent*-kauranes. *J. Nat. Prod.* **2007**, *70*, 347–352. [[CrossRef](#)] [[PubMed](#)]
27. Chen, K.; Shi, Q.; Fujioka, T.; Zhang, D.C.; Hu, C.Q.; Jin, J.Q.; Kilkuskie, R.E.; Lee, K.H. Anti-AIDS agents, 4. Tripterifordin, a novel anti-HIV principle from *Tripterogium wilfordii*: Isolation and structural elucidation. *J. Nat. Prod.* **1992**, *55*, 88–92. [[CrossRef](#)] [[PubMed](#)]
28. Chang, F.R.; Yang, P.Y.; Lin, J.Y.; Lee, K.H.; Wu, Y.C. Bioactive kaurane diterpenoids from *Annona glabra*. *J. Nat. Prod.* **1998**, *61*, 437–439. [[CrossRef](#)] [[PubMed](#)]
29. Wu, Y.C.; Hung, Y.C.; Chang, F.R.; Cosentino, M.; Wang, H.K.; Lee, K.H. Identification of *ent*-16 $\beta$ ,17-dihydroxykauran-19-oic acid as an anti-HIV principle and isolation of the new diterpenoids annosquamosins A and B from *Annona squamosal*. *J. Nat. Prod.* **1996**, *59*, 635–637. [[CrossRef](#)] [[PubMed](#)]
30. Sun, H.D. *Diterpenoid Chemistry (Ertie Huaxue)*; Chemical Industry Press: Beijing, China, 2011; p. 206.
31. Sheldrick, G.M. *SHELXL-97, Program for X-ray Crystal Structure Refinement*; University of Gottingen: Gottingen, Germany, 1997.

32. Zhang, H.J.; Ma, C.Y.; Hung, N.V.; Cuong, N.M.; Tan, G.T.; Santarsiero, B.D.; Mesecar, A.D.; Soejarto, D.D.; Pezzuto, J.M.; Fong, H.H.S. Miliusanes, a class of cytotoxic agents from *Miliusa sinensis*. *J. Med. Chem.* **2006**, *49*, 693–708. [[CrossRef](#)] [[PubMed](#)]
33. O'Toole, G.A.; Kolter, R. Initiation of biofilm formation in *Pseudomonas fluorescens* WCS365 proceeds via multiple, convergent signaling pathways: A genetic analysis. *Mol. Microbiol.* **1998**, *28*, 449–461. [[CrossRef](#)] [[PubMed](#)]
34. Koneman, E.W.; Allen, S.D.; Janda, W.M.; Schreckenberger, P.C.; Winn, W.C. *Color Atlas And Textbook of Diagnostic Microbiology*, 5th ed.; Lippincott: Philadelphia, PA, USA, 1997; pp. 803–841.
35. Yang, H.C.; Mikami, Y.; Yazawa, K.; Taguchi, H.; Nishimura, K.; Miyaji, M.; Branchini, M.L.; Aoki, F.H.; Yamamoto, K. Colorimetric MTT assessment of antifungal activity of D0870 against fluconazole-resistant *Candida albicans*. *Mycoses* **1998**, *41*, 477–480. [[CrossRef](#)] [[PubMed](#)]
36. CLSI. *Reference Method for Broth Dilution Antifungal Susceptibility Testing of Filamentous Fungi, Approved Standard, CLSI document M38-A2*, 2nd ed.; Clinical and Laboratory Standards Institute: Wayne, PA, USA, 2008.
37. He, J.; Choe, S.; Walker, R.; di Marzio, P.; Morgan, D.O.; Landau, N.R. Human immunodeficiency virus type I viral protein R (Vpr) arrests cells in the G2 phase of the cell cycle by inhibiting p34cdc2 activity. *J. Virol.* **1995**, *69*, 6705–6711. [[PubMed](#)]
38. Connor, R.I.; Chen, B.K.; Choe, S.; Landau, N.R. Vpr is required for efficient replication of human immunodeficiency virus type-1 in mononuclear phagocytes. *Virology* **1995**, *206*, 935–944. [[CrossRef](#)] [[PubMed](#)]



© 2015 by the authors; licensee MDPI, Basel, Switzerland. This article is an open access article distributed under the terms and conditions of the Creative Commons by Attribution (CC-BY) license (<http://creativecommons.org/licenses/by/4.0/>).